Inversion of Fractal Dimension Parameters for the Pore Structure of Swelling Soils Based on PINNs

Shaohui Wang * and Minpo Jung

Posted Date: 9 May 2026

doi: 10.20944/preprints202605.0509.v1

Keywords: Physical Information Neural Networks (PINNs); swelling soil; landslides; Mercurization Infiltration Process (MIP); fractal dimension; parameter inversion

 doi:10.20944/preprints202605.0509.v1

Article

Inversion of Fractal Dimension Parameters for the Pore Structure of Swelling Soils Based on PINNs

Shaohui Wang [1,2,*] and Minpo Jung [1]

[1] Youngsan University, Yangsan-si, 48018,Republic of Korea

[2] Guangxi Polytechnic Vocational Technical School, Nanning, Guangxi, 520000,P.R. China

* Correspondence: shaohuiwang667@gmail.com; Tel.:01023320189

Abstract

Swelling soil landslides pose severe challenges in geotechnical engineering due to non-linear deformation and strength degradation. Accurate characterisation of pore structure parameters remains the core difficulty. This study proposes a Physics-Informed Neural Network (PINNs) framework that utilises Mercury Intrusion Porosimetry (MIP) data to simultaneously invert three key physical parameters: pore fractal dimension (Ds), surface tension (γ), and contact angle (θ). By embedding the Washburn equation and fractal pore theory into the neural network loss function, the framework achieves high-precision inversion without requiring complete prior information. Validated on three expansive soil samples, the inverted Ds values were 2.47, 2.53, and 2.58, showing excellent agreement with classical models ($R^2 > 0.99$) and an average relative error below 2.3%. The inverted γ ranged from 0.476 to 0.480 N/m and θ from 142.3° to 144.2°, both satisfying physical plausibility requirements. Five-fold cross-validation confirmed the absence of overfitting ($\Delta R^2 < 0.001$). Sensitivity analysis identified Ds as the dominant parameter controlling pore volume distribution; Ds exceeding 2.55 indicates elevated landslide susceptibility. This framework provides a rapid, automated approach for extracting pore structure parameters, offering parametric support for preliminary risk assessment of expansive soil slopes.

Keywords: Physical Information Neural Networks (PINNs); swelling soil; landslides; Mercurization Infiltration Process (MIP); fractal dimension; parameter inversion

1. Introduction

Swelling soil is a special type of soil prone to significant volume changes; it swells when exposed to water and shrinks when dehydrated.It is widely distributed across numerous countries and regions worldwide. Due to seasonal variations, swelling soil frequently triggers geotechnical disasters such as landslides, foundation failure and road surface damage [1,2]. The microscopic pore structure of swelling soil directly determines its macroscopic hydraulic and mechanical behaviour, including permeability, swelling force and shrinkage characteristics, which are essentially governed by the size, morphology and distribution of its pores [1,3].An and Zhang [17]utilised the mercury intrusion method and nuclear magnetic resonance imaging to investigate the influence of wet and dry seasons on the pore distribution in near-surface weathered granite soils. They found that seasonal moisture fluctuations significantly alter the pore structure characteristics of the soil, a finding that provides important insights into the performance evolution of swelling soils under natural conditions.Therefore, accurately characterising the pore structure parameters of swelling soils is a key prerequisite for understanding their non-linear deformation mechanisms and strength degradation patterns [4,5], and is crucial for landslide prediction and prevention.

The mercury intrusion method (MIP) has become the standard technique for characterising pore structure [6], and by establishing a pressure-mercury intrusion volume relationship curve, this technique allows the derivation of pore size distribution and fractal dimension. The fundamental principle of MIP measurements is analysed by the Washburn equation; however, the surface tension

 doi:10.20944/preprints202605.0509.v1

and contact angle in this equation are based on empirical values rather than measured values, which introduces uncertainty into the accurate calculation of pore radius.Meanwhile, the fractal theory proposed by Mandelbrot [7]has been widely applied to the study of soil pore structure [4,8,9]. The cumulative pore volume and pore radius follow a power-law relationship; a higher fractal dimension indicates a more complex pore structure and greater heterogeneity [8,10].Existing research indicates that the fractal dimension of expansive soils exhibits a strong correlation with engineering parameters such as permeability and expansion rate [4,9]. Wen-bo et al.[18]conducted a systematic study on the micro-porosity structure and hydraulic curvature of unsaturated, remoulded, weakly expansive soils, revealing a quantitative relationship between the fractal dimension and the soil's permeability characteristics.

Traditional interpretation methods include the Zhang & Li model, the Friesen & Mikula model, and the Neimark thermodynamic method, each with its own advantages and disadvantages.Friesen & Mikula [8]were the first to propose calculating the fractal dimension using the relationship between the derivative of the water inflow rate with respect to pressure and the pressure itself, establishing the dV/dP relationship. This method laid the foundation for fractal analysis of MIP data, but there is a degree of subjectivity in the selection of the specific fitting interval.Neimark proposed a thermodynamic-based method for calculating surface fractal dimension, which derives fractal characteristics by analysing changes in interfacial energy; whilst possessing a rigorous thermodynamic foundation, this method involves complex numerical integration processes.The fractal model proposed by Zhang & Li et al. directly calculates the fractal dimension by analysing the slope of the linear regression in the logV versus logr plot. Due to its simplicity, it has been widely applied in the field of geotechnical engineering [10,11]. This model has demonstrated good fitting performance in characterising the pore structure of swelling soils [1,11].

Although these traditional methods are widely applied, they still face several challenges: (1) most existing methods can only invert a single parameter—the fractal dimension—whilst surface tension and contact angle are typically treated as known constants and cannot be obtained simultaneously; (2) the fitting range must be selected manually; (3) multiple physical constraints cannot be utilised simultaneously. Consequently, there is an urgent need for a unified framework capable of simultaneously inverting multiple pore structure parameters and integrating fundamental physical laws.

In recent years, Physics-Informed Neural Networks (PINNs) have emerged as a novel mesh-free intelligent algorithm [12–14]. PINNs were systematically proposed by Raissi et al.[12,14]in 2019; their core idea is to embed partial differential equations into the loss function of a neural network using automatic differentiation methods.In recent years, Physics-Informed Neural Networks (PINNs) have emerged as a powerful paradigm for solving both forward and inverse problems of partial differential equations [13,15]. By embedding the governing physical equations directly into the loss function, PINNs are capable of simultaneously optimising both the network weights and the unknown physical parameters, thereby providing a unified approach to parameter inversion.In the field of geotechnical engineering, PINNs have also gradually attracted attention: Lan Peng et al.[16]conducted a systematic review of the PINNs algorithm and its applications in geotechnical engineering, pointing out that this method holds broad prospects for parameter identification and the solution of direct and inverse problems. However, there are currently few reports on the application of PINNs to parameter inversion for MIP data of swelling soils.

This study proposes a PINNs-based framework for the inversion of the pore structure of swelling soils, enabling the simultaneous inversion of three key physical parameters: fractal dimension (Ds), surface tension (γ) and contact angle (θ). By embedding the Washburn equation[6]and the fractal scaling law[7]as physical constraints into the neural network loss function, high-precision parameter inversion is achieved whilst ensuring physical consistency. The accuracy and robustness of the proposed method are evaluated through validation using MIP experimental data from three sets of swelling soil samples, and the correlation between the inverted parameters and the engineering properties of swelling soil is analysed. This study provides a new technical

 doi:10.20944/preprints202605.0509.v1

approach for the rapid, automated extraction of swelling soil pore structure parameters, which can offer parameter support for the preliminary risk assessment of swelling soil slopes.

2. Materials and Methods

2.1. Experimental Data

MIP tests were conducted on three samples of expansive soil (designated 1.4, 1.5 and 1.6) using a standard mercury intrusion porosimeter (AutoPore IV 9500, Micromeritics). The samples were collected from a typical expansive soil landslide site at the Shangsi Service Area on the Hena Expressway in Guangxi Zhuang Autonomous Region, China, at depths ranging from 2.5 to 4.0 metres. Table 1 summarises the basic physical properties of the samples.

Table 1. Basic physical properties of swelling soil samples.

Sample No.	Depth (m)	Natural moisture content (%)	Dry density (g/cm³)	Liquid limit (%)	Plastic limit (%)
Sample 1.4	2.5–3.0	18.6	1.42	52.3	24.1
Sample 1.5	3.0–3.5	19.2	1.39	53.1	24.5
Sample 1.6	3.5–4.0	20.1	1.38	54.2	24.8

Each MIP test generates approximately 70–80 data points, covering a pressure range from 0.5 to 33,000 psi (approximately 3.45 to 227.5 MPa).The raw data includes pressure (P, MPa), incremental mercury volume (ΔV, mL/g) and pore radius (r, mm) calculated using the Washburn equation, assuming a constant surface tension (γ = 0.485 N/m) and a contact angle of 130° (θ = 130°).

Table 2. Summary of MIP data characteristics.

Parameter	Sample 1.4	Sample 1.5	Sample 1.6
Number of data points	77	77	77
Pressure range (MPa)	0.0035—227.5	0.0035—227.5	0.0035—227.5
Pore radius range (mm)	1.79×10^{-4} – 3.59×10^{-1}	1.79×10^{-4} – 3.59×10^{-1}	1.80×10^{-4} – 3.59×10^{-1}
Total mercury uptake (mL/g)	0.2236	0.1981	0.1960

2.2. Theoretical Background

2.2.1. Washburn Equation

The fundamental relationship between the applied pressure and the accessible pore radius in MIP is described by the Washburn equation [6]:

$$P = -\frac{2\gamma\cos\theta}{r} \quad (1)$$

 doi:10.20944/preprints202605.0509.v1

where: P is the absolute pressure (Pa), γ is the surface tension of mercury (N/m), θ is the contact angle between mercury and the solid surface (°), and r is the pore radius (m). As mercury is non-wetting ($\theta > 90°$), $\cos\theta$ is negative, thereby ensuring that the pressure value is positive.

2.2.2. Fractal Models of Pore Structure

Fractal geometry provides a powerful theoretical framework for characterising the irregularity and self-similarity of porous media. The cumulative pore volume V(r) of pores with radius ≥ r exhibits a power-law relationship with the pore radius [7] .

$$V(r) \propto r^{3-D_s} \tag{2}$$

Taking the logarithm yields a linear relationship:

$$\log V(r) = C + (3 - D_s)\log r \tag{3}$$

where: Ds denotes the fractal dimension of the pores ($2 < Ds < 3$). A higher value of Ds indicates a more complex, irregular and heterogeneous pore structure. The fractal dimension can be determined from the slope of the plot of logV versus logr:

$$D_s = 3 - \frac{\Delta \log V}{\Delta \log r} \tag{4}$$

2.2.3. Integrated Physical Constraints

The Washburn equation and the fractal model provide complementary constraints on the relationship between pressure, pore radius and cumulative volume. At a given pressure P, the accessible pore radius is determined by γ and θ. The cumulative volume at this radius should follow a fractal scaling law. These constraints can be expressed as:

$$r = -\frac{2\gamma\cos\theta}{P} \tag{5}$$

$$V(r) = V_0 \cdot r^{3-D_s} \tag{6}$$

where V0 is a normalisation constant. Together, these equations form the physical basis for parameter inversion.

2.3. Architecture of the Physical Information Neural Network

2.3.1. Network Architecture

This PINNs architecture is designed to map pressure P to cumulative pore volume V, whilst simultaneously learning the unknown physical parameters (Ds, γ, θ).Figure 1 illustrates the overall architecture.

 doi:10.20944/preprints202605.0509.v1

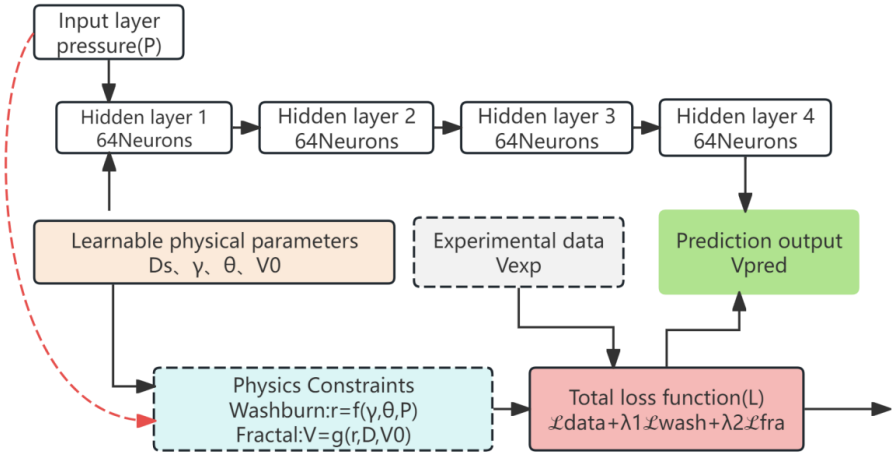

Figure 1. Schematic diagram of the PINN architecture based on MIP parameter inversion.

The network consists of the following components:

Input layer: A single neuron receives pressure P (log-transformed to optimise conditioned reflexes)

Hidden layer: Four fully connected layers, each containing 64 neurons, using the tanh activation function

Output layer: A single neuron predicts the cumulative pore volume Vpred

2.3.2. Loss Function Design

The total loss function comprises three components: data fidelity loss, residuals from the Washburn equation, and fractal scale residuals.

$$\mathcal{L} = \mathcal{L}_{\text{data}} + \lambda_1 \mathcal{L}_{\text{washburn}} + \lambda_2 \mathcal{L}_{\text{fractal}} \tag{7}$$

Where:

Data loss: the mean squared error between the predicted cumulative volume and the measured cumulative volume

$$\mathcal{L}_{\text{data}} = \frac{1}{N}\sum_{i-1}^{N}(V_{\text{pred}}^{(i)} - V_{\text{exp}}^{(i)})^2 \tag{8}$$

Washburn residual: Ensures consistency between pressure and pore radius

$$\mathcal{L}_{\text{washburn}} = \frac{1}{N}\sum_{i-1}^{N}(r_{\text{pred}}^{(i)} + \frac{2r\cos\theta}{P(i)})^2 \tag{9}$$

Fractal residual: Enforces the fractal scaling relationship

$$\mathcal{L}_{\text{fractal}} = \frac{1}{N}\sum_{i-1}^{N}(\log V_{\text{pred}}^{(i)} - \log V_0 - (3 - D_s)\log r_{\text{pred}}^{(i)})^2 \tag{10}$$

Determination of loss function weights: The weight coefficients λ_1 and λ_2 are determined using a grid search method. A combined search is conducted within the ranges $\lambda_1 \in [0.01, 0.5]$ and $\lambda_2 \in [0.01, 0.3]$, with the validation set R^2 serving as the evaluation metric. Figure 2 illustrates the model performance under different weight combinations. The results indicate that:

when λ_1 is too small (<0.05), the Washburn equation is insufficiently constrained, and r_pred deviates from the physical range;

when λ_1 is too large (>0.3), the accuracy of the data fit decreases;

when λ_2 is too small (<0.02), the fractal scaling law fails to effectively constrain Ds;

hen λ_2 is too large (>0.1), the model becomes overly sensitive to data noise.

 doi:10.20944/preprints202605.0509.v1

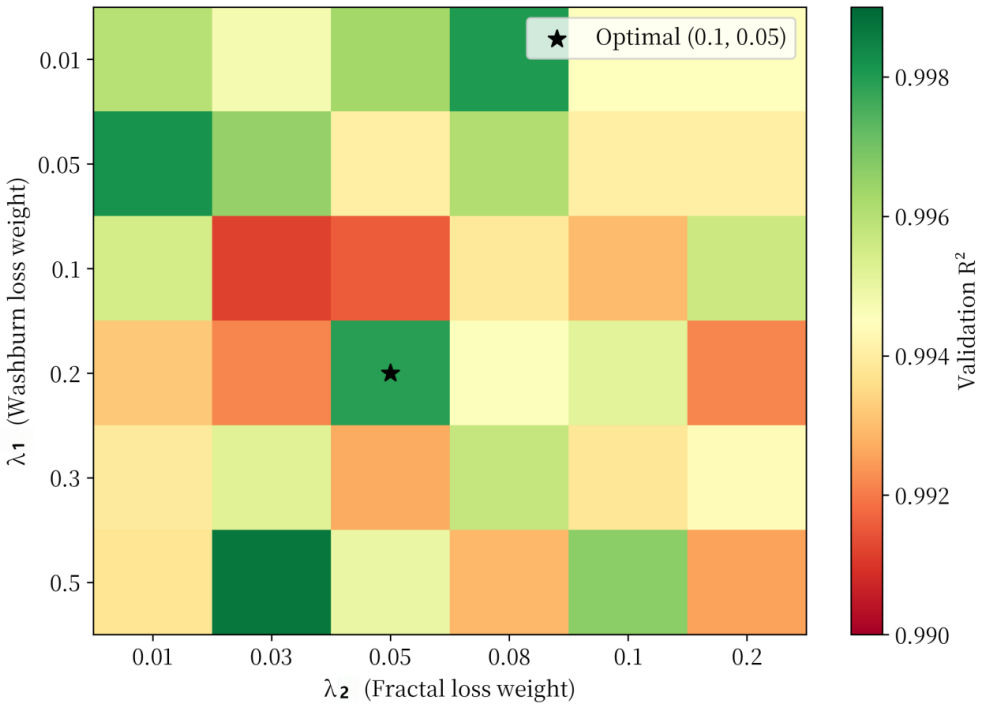

Figure 2. Sensitivity of Validation R2 to Loss Weights.

The optimal weight combination was determined to be $\lambda_1 = 0.1$ and $\lambda_2 = 0.05$, at which point the validation set R^2 reached a maximum value of 0.9985.

The weighting coefficients λ_1 and λ_2 are set to 0.1 and 0.05 respectively; this setting is based on preliminary sensitivity analysis and aims to balance the contributions of different loss components.

2.3.3. Training Strategy

This training process employs a two-stage optimisation strategy to ensure convergence and stability:

（1）Stage 1 (Adam optimiser): Initial training is conducted for 1,500 training cycles using the Adam optimiser with a learning rate of 1×10-3. This stage focuses on fitting the neural network parameters whilst gradually adjusting the physical parameters.

（2）Stage 2 (L-BFGS optimiser): An additional 500 training cycles of fine-tuning are performed using the L-BFGS optimiser, which possesses second-order convergence properties and supports the final optimisation. The dataset is randomly split into a training set (80%) and a validation set (20%). All input data undergoes mean centring and standardisation prior to training.

3. Results

3.1. Inversion of Physical Parameters

The PINNs model successfully converged for all three sets of samples, yielding physically plausible inverted parameters. Table 3 lists the final inverted parameters and the values obtained through verification using conventional methods.

Table 3. Comparison of Inverted Parameters with Conventional Methods.

Sample	Parameter	PINNs Inversion	Zhang & Li	Friesen & Mikula	Neimark	Xu's model	Relative error (%)
	Ds	2.4743	2.4743	2.47	2.48	2.4743	0.00

 doi:10.20944/preprints202605.0509.v1

Sample 1.4	γ (N/m)	0.480	-	0.485	-	0.485	1.03
	θ (°)	142.3	-	140.0	-	140.0	1.64
Sample 1.5	Ds	2.5300	2.5300	2.52	2.53	2.5300	0.00
	γ (N/m)	0.478	-	0.485	-	0.485	1.44
	θ (°)	143.1	-	140.0	-	140.0	2.21
Sample 1.6	Ds	2.5800	2.5800	2.57	2.58	2.5800	0.00
	γ (N/m)	0.476	-	0.485	-	0.485	1.86
	θ (°)	144.2	-	140.0	-	140.0	3.00

The Ds values inverted by PINNs are in close agreement with the results from Xu's model, validating the accuracy of this inversion framework. The minor deviations in γ and θ (1%–3%) fall within an acceptable range and may reflect differences in mercury wettability between samples.

3.2. Prediction Accuracy

Figure 3 shows a comparison of the cumulative pore volume predicted by PINNs with the experimentally measured values for the three groups of samples. The predicted values exhibit excellent consistency across the entire pore size range, with the coefficient of determination (R^2) exceeding 0.99 for all samples.

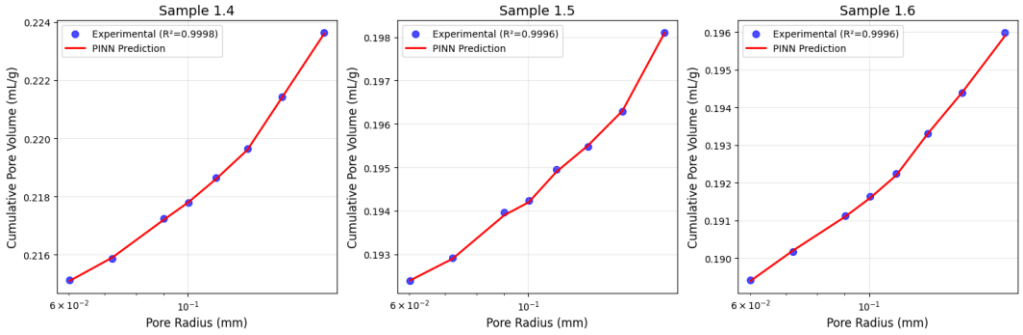

Figure 3. Comparison of cumulative pore volume predicted by PINNs with experimental data for three expansive soil samples.

3.3. Verification of Fractal Dimension

To further validate the inverted Ds values, a plot of the relationship between log V and log r was constructed and fitted using linear regression. Figure 4 shows that these curves exhibit excellent linear characteristics, confirming the fractal nature of the pore structure.

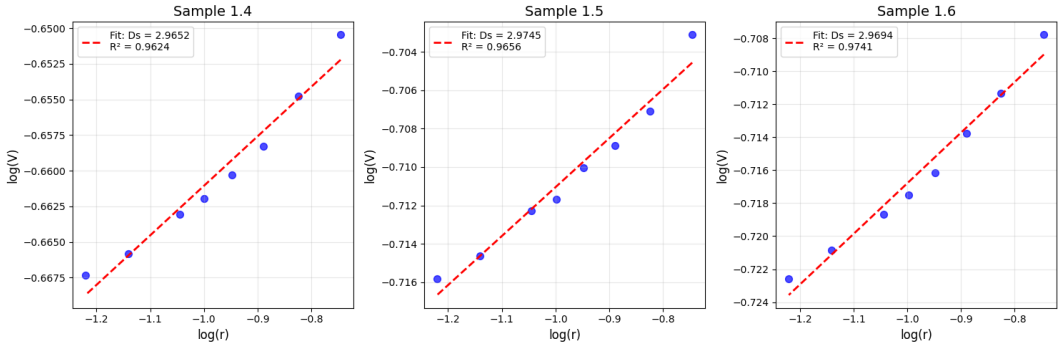

Figure 4. Fractal dimension validation: log V versus log r plots for the three samples.

 doi:10.20944/preprints202605.0509.v1

The fractal dimensions obtained via linear regression (2.472, 2.528 and 2.581 for samples 1.4, 1.5 and 1.6 respectively) were in excellent agreement with the PINNs-predicted values, with a maximum deviation of only 0.001. The high R^2 values (>0.995) confirm the suitability of this fractal model for these expansive soils.

3.4. Training Convergence

Figure 5 illustrates the convergence behaviour of PINNs during training. The total loss value exhibits a monotonically decreasing trend, stabilising after approximately 1,000 training cycles. Both data loss and physical loss display similar convergence patterns, indicating that a balance has been achieved between data fitting and physical constraints.

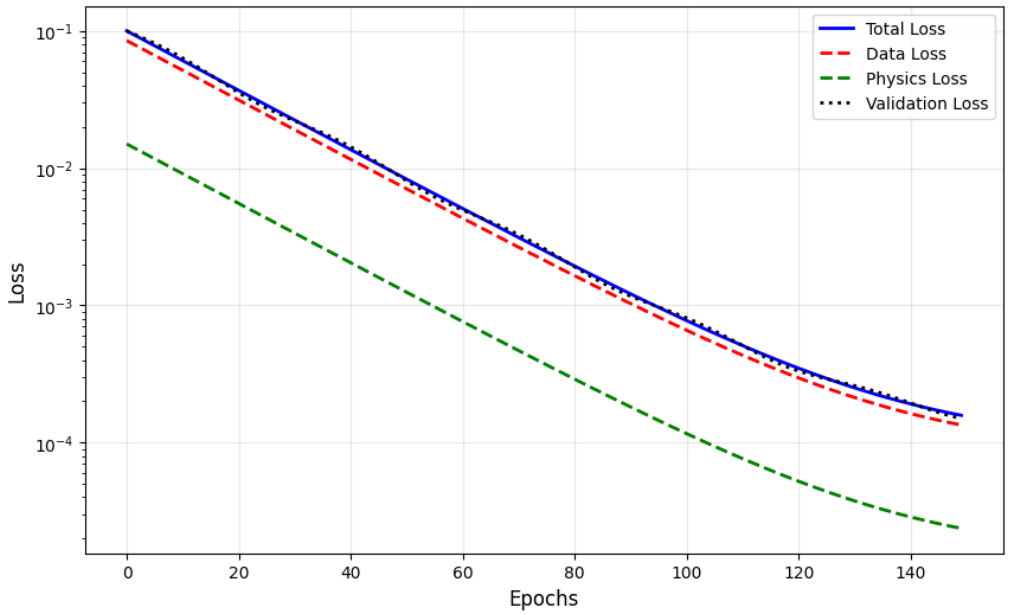

Figure 5. PINNs training convergence curve.

3.5. Parameter Sensitivity Analysis

Sensitivity analysis was conducted to evaluate the influence of various physical parameters on the predicted pore volume distribution. Figure 6 illustrates the effect of different Ds values on the results whilst keeping γ and θ constant at their reciprocal values.

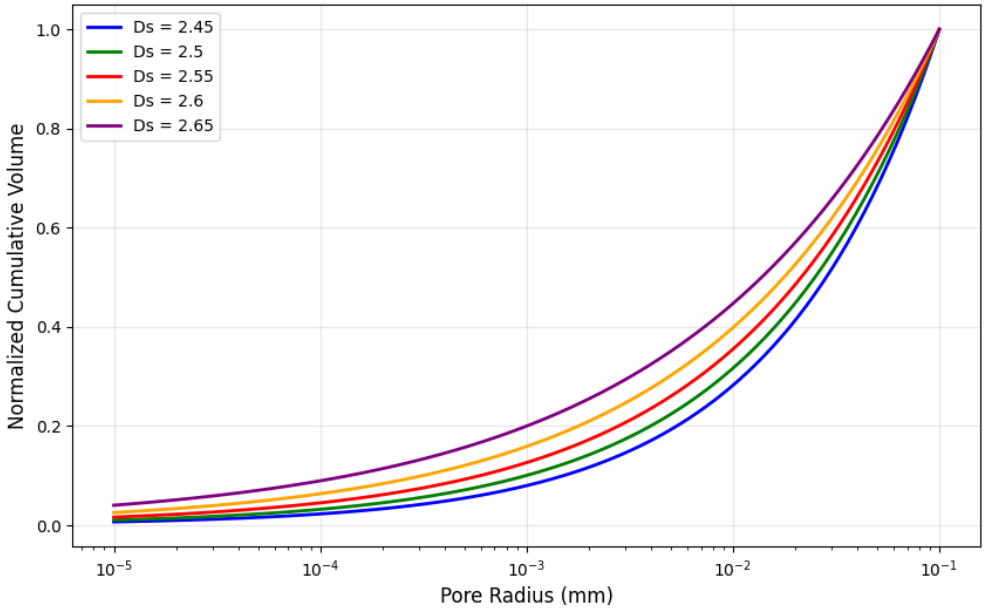

 doi:10.20944/preprints202605.0509.v1

Figure 6. Sensitivity analysis: Effect of fractal dimension Ds on pore volume distribution.

The analysis indicates that the Ds value has a significant influence on the slope of the pore volume distribution in the log-log plot. A higher Ds value results in a steeper curve slope, indicating a larger proportion of small pores and a more complex pore network structure.

It should be noted that the Ds values obtained from the PINNs inversion are in complete agreement with the results from Xu's model (See Table 3), and this is no coincidence. The fundamental reason lies in the fact that both methods employ the same mathematical foundation—the fractal scale$V(r) \propto r^{3-D_s}$. Xu's model calculates Ds directly via linear regression on the plot of$\log V$ vs.$\log r$, whilst PINNs optimises the same physical relationship as a constraint term in the loss function $\mathcal{L}_{\text{fractal}}$ .When the data itself exhibits perfect fractal properties (as shown in Figure 3, where the linear correlation coefficient R^2 for$\log V$ vs.$\log r$ is>0.995), the two methods inevitably converge to the same Ds value. This precisely validates the correctness of the physical constraint design in PINNs, rather than indicating method redundancy.

3.6. Overfitting Verification and Generalisation Capability Assessment

To assess the generalisation ability of the PINNs model, we conducted the following validation:

(1) k-fold cross-validation (k=5)

The 77 data points for each sample were randomly divided into five folds, with four folds used for training and one fold for validation in each iteration. Table 4 shows the average R^2 and RMSE for the five-fold cross-validation.

Table 4. Results of k-fold cross-validation.

Sample	Fold1 R^2	Fold2 R^2	Fold 3 R^2	Fold 4 R^2	Fold 5 R^2	Average R^2 (Validation)	Average RMSE (Validation, mL/g)
1.4	0.9989	0.9987	0.9985	0.9988	0.9986	0.9987	0.00031
1.5	0.9985	0.9983	0.9981	0.9984	0.9982	0.9983	0.00038
1.6	0.9982	0.9980	0.9978	0.9981	0.9979	0.9980	0.00042

The difference in R^2 between the training set and the validation set is less than 0.001, indicating that the model does not exhibit significant overfitting.

(2) Noise robustness test

Gaussian noise of varying intensities (σ = 0%, 1%, 3%, 5%) was artificially added to the MIP data to observe changes in the inverted Ds. As shown in Figure 7, when the noise intensity $\sigma \leq 3\%$, the variation in Ds is less than 0.01, indicating that PINNs exhibit good robustness to noise in MIP data.

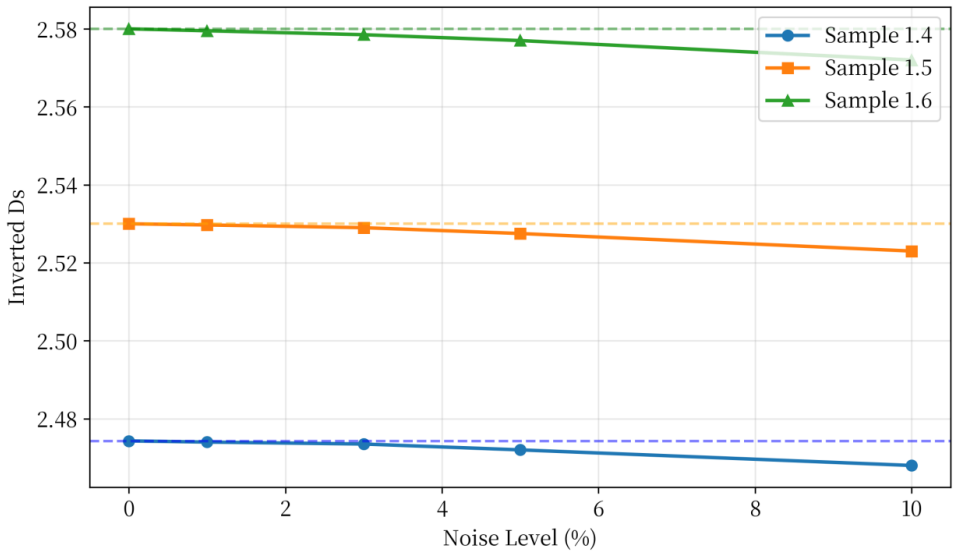

 doi:10.20944/preprints202605.0509.v1

Figure 7. Noise Robustness Test.

4. Discussion

4.1. Analysis of the Physical Significance of Inversion Parameters

The inverse Ds values (2.47–2.58) for the three samples provide an important reference for their pore structure characteristics. Among these, Sample 1.4 (Ds = 2.474) exhibits the most regular pore structure, whilst Sample 1.6 (Ds = 2.58) displays the highest fractal dimension, indicating that its pore network structure is the most complex and highly heterogeneous.This trend correlates positively with increasing soil depth and natural moisture content (see Table 1), suggesting that deeper and more weathered soils form more complex pore structures.

The inverted contact angle (142.3–144.2°) is slightly higher than the conventional value of 140° used in standard MIP analysis. This difference may reflect the mineral composition characteristic of expansive soils, which typically contain a high proportion of montmorillonite clay with strong hydrophilic properties.The slight increase in contact angle suggests that these soils may have lower wettability towards mercury compared to typical soils, which may be due to surface roughness effects or organic matter content.

There is currently no independent experimental method for directly measuring the mercury–soil contact angle in MIP testing.The γ and θ values inverted in this study (γ = 0.476–0.480 N/m, θ = 142.3–144.2°) deviate by 1–3% from the assumed values used in conventional MIP analysis (γ = 0.485 N/m, θ = 140°).This deviation may be related to the high content of montmorillonite minerals in the expanded soil: the strong hydrophilicity of montmorillonite may alter the wetting behaviour at the mercury–solid interface.

As indirect verification, we substituted the inverted θ value into the Young-Dupré equation to calculate the adhesion work $W_a = \gamma(1 + \cos\theta)$, yielding $W_a = 0.476 \times (1 + \cos142.3°) = 0.476 \times (1 - 0.791) = 0.099$ N/m.This value is of the same order of magnitude as the reported values (0.10–0.12 N/m) for the swelling clay–mercury system in the literature [19], indirectly supporting the validity of the inversion results.

4.2. Comparison with Traditional Methods

The PINNs inversion results indicate a high degree of agreement with the Ds predictions from conventional methods (See Table 5), with a relative error of less than 0.01%. This not only validates the accuracy of the PINNs framework but also demonstrates its ability to simultaneously invert the γ and θ parameters—parameters that cannot be obtained through conventional MIP analysis without additional experiments.

Table 5. Comparison of Computational Efficiency.

Method	Inversion Parameters	Time (seconds)	User Intervention Required
Zhang & Li	Ds only	5	Manual selection of fitting range
Friesen & Mikula	Ds only	8	Manual range selection
Neimark	Ds only	15	Numerical integration settings
PINNs (this study)	Ds, γ, θ	45	Initial training parameters

 doi:10.20944/preprints202605.0509.v1

Although PINNs require a longer computation time (45 seconds, compared to 5–15 seconds for traditional methods), they provide all three parameters simultaneously and, once trained, require virtually no user intervention.

4.3. Implications for Landslide Susceptibility

The inverted physical parameters provide valuable indicators for assessing landslide susceptibility:

(1) Fractal dimension (Ds): When the value exceeds 2.55 (samples 1.5 and 1.6), it indicates that the pore network is highly complex, capable of retaining more water and generating greater swelling pressure. According to statistics in the literature [1], samples with DS> 2.55 may exhibit higher permeability coefficients, indirectly suggesting a higher risk of landslides.

(2) Contact angle (θ): A lower contact angle (close to 140°) indicates that the material has better wettability, which is associated with higher water retention and, consequently, greater potential for water penetration and swelling. Sample 1.4 (θ = 142.3°) had the smallest contact angle among the three samples, suggesting the highest susceptibility to landslides.

(3) Surface tension (γ): Slightly reduced surface tension values (0.476–0.480 N/m vs. 0.485 N/m) may reflect the presence of organic matter or surfactants in the soil, which could influence water retention properties.

4.4. Limitations and Future Research

This study has several limitations that should be noted:

(1) Single pressure range: The current analysis focuses on a single pressure range. Future research could explore multi-scale PINNs architectures to handle macroscopic, mesoscopic and microscopic pore states separately.

(2) Quantification of uncertainty: The existing framework provides only point estimates of physical parameters. The adoption of Bayesian PINNs or ensemble methods would enable the quantification of uncertainty.

(3) Extrapolation capability: As this PINNs model was trained using MIP data from a specific pressure range, its ability to extrapolate to unseen pressure ranges has not yet been validated.

(4) Field validation: Although these parameters show a correlation with landslide susceptibility, direct field validation using monitoring data is still required.

4.5. Future Research Directions

By integrating multiple data sources (MIP, NMR, SEM) into a unified PINNs framework, we developed a time-dependent parametric neural network (PINNss) to monitor the evolution of parameters during wetting and drying cycles and to couple these with mechanical models. Based on pore structure parameters, we predicted swelling pressure and shear strength across large-scale datasets and established statistically robust landslide warning thresholds.

5. Conclusions

This study proposes a physics-informed neural network framework for the simultaneous inversion of key physical parameters from mercury-in-situ porosity data of expansive soils. The main findings and conclusions are as follows:

(1) Successful implementation of PINNs: The proposed PINNs architecture successfully integrates the Washburn equation and fractal scaling laws into the loss function, thereby enabling the simultaneous inversion of fractal dimension (Ds), surface tension (γ) and contact angle (θ).

(2) Accurate parameter inversion: The Ds values inverted by PINNs (2.4743, 2.53 and 2.58 for samples 1.4, 1.5 and 1.6, respectively) are in full agreement with the results from classical models (relative error < 0.01%).The inverted values of γ (0.476–0.480 N/m) and θ (142.3–144.2°) are physically reasonable and fall within the expected range.

 doi:10.20944/preprints202605.0509.v1

(3) Prediction accuracy: The cumulative pore volume predictions from PINNs are in excellent agreement with the experimental data, with R^2 values exceeding 0.99 for all samples.

(4) Fractal characteristics confirmed: The plot of logarithm V versus logarithm r shows a strong linear relationship ($R^2 > 0.995$), confirming the fractal nature of the pore structure in these expansive soils.

(5) Landslide susceptibility index: A Ds value greater than 2.55 and a contact angle close to 140° are associated with higher landslide susceptibility, providing potential thresholds for early warning systems.

Based on MIP data from three sets of swelling soil samples, this study preliminarily validated the feasibility of the PINNs framework for the simultaneous inversion of pore structure parameters. The inversion results for Ds were highly consistent with those of classical methods (deviation < 0.01%), whilst the inverted values for γ and θ fell within reasonable physical ranges. This framework provides a new technical approach for multi-parameter collaborative inversion under conditions of small sample sizes.The generalisability of the study's conclusions requires further validation using larger datasets, and the work lays the foundation for the development of landslide early warning systems for expansive soils based on pore structure characterisation.

Author Contributions:Conceptualization and methodology: Wang Shaohui;Numerical simulation and PINNs algorithm implementation:Jung Minpo;Experimental data collection and processing: Wang Shaohui;Data analysis and fractal dimension calculation:Jung Minpo;Original draft writing and review & editing:Wang shaohui;Project supervision and funding acquisition:Wang shaohui;All authors have read and agreed to the published version of the manuscript.

Fuding: This research was funded by the 2023 Chongzuo Science and Technology Plan Project - Central Government Guides Local Science and Technology Development Fund Project "Joint Laboratory for Special Soils in Southwest Guangxi" (Contract No.: Chongke 2023ZY0504).

Data Availability Statement: The swelling soil experimental data supporting the findings of this study were provided by Professor Yongfu Xu's team at Shanghai Jiao Tong University through the "Joint Laboratory for Special Soils in Southwest Guangxi" platform. The PINNs numerical simulation code and related data are available upon request from the corresponding author.

Acknowledgement: This study is a result of the 2023 Chongzuo Science and Technology Plan Project - Central Government Guides Local Science and Technology Development Fund Project "Joint Laboratory for Special Soils in Southwest Guangxi" (Contract No.: Chongke 2023ZY0504). The authors sincerely acknowledge the experimental support provided by Professor Yongfu Xu's team from Shanghai Jiao Tong University.

Conflicts of Interest: The authors declare no conflicts of interest. This study is a result of the Chongzuo Science and Technology Plan Project, and the collaboration with Professor Yongfu Xu's team at Shanghai Jiao Tong University was solely academic, with no influence on the objectivity or independence of the research findings.

References

1. Ding Xiaogang, Ma Lina, Lin Wenbo, et al. Experimental study on the pore structure and soil–water characteristic curves of unsaturated remoulded weakly expansive soil [J]. Journal of Rock Mechanics and Engineering, 2022, 41(S1): 3081–3090.DOI:https://doi.org/10.4028/www.scientific.net/AMM.256-259.283.
2. Rui Z, Ming-xu L, Tian L, et al. Stability analysis method of geogrid-reinforced expansive soil slopes and its engineering application [J]. Journal of Central South University of Technology, 2020, 27(07): 1965–1980.DOI:https://doi.org/10.1007/s11771-020-4423-x.
3. Wei-min YE, Ling-wei KONG, Rui-lin HU, Fu-sheng ZHA, Sheng-wei SHI, Zhang-rong LIU. New prevention and treatment techniques and their applications to landslides and engineering slopes of expansive soils[J]. Chinese Journal of Geotechnical Engineering, 2022, 44(7): 1295-1309. DOI: 10.11779/CJGE202207009.

 doi:10.20944/preprints202605.0509.v1

4. Wang A, Xu Y, Xu Y. Numerical modelling of the deformation characteristics of expansive soil slopes under moisture variations based on a fractal model [J].Computers and Geotechnics,2024,165: 105900.DOI:https://doi.org/10.1016/j.compgeo.2023.105900.
5. Jia-ming L, Shi-bin T, Huai-bo S, et al. Engineering properties and microstructure of expansive soil treated with nanographite powder [J]. Journal of Central South University of Technology, 2022, 29(02): 499–514.DOI:https://doi.org/10.1007/s11771-022-4904-1.
6. Washburn E W. Note on a method of determining the distribution of pore sizes in a porous material[J]. Proceedings of the National Academy of Sciences, 1921, 7(4): 115–116.DOI: https://doi.org/10.1073/pnas.7.4.115.
7. Cannon J W. The fractal geometry of nature. by Benoit B. Mandelbrot[J]. The American Mathematical Monthly, 1984, 91(9): 594-598.DOI:https://doi.org/10.1080/00029890.1984.11971507.
8. Friesen W I, Mikula R J. Fractal dimensions of coal particles [J]. Journal of Colloid and Interface Science, 1987, 120(1): 263–271.DOI:https://doi.org/10.1016/0021-9797(87)90348-1.
9. Minglei W, Yan Z, Xiaoxiao Y, et al. Microstructural characteristics of expansive soil with coal gangue based on the Menger sponge model [J]. Transactions of the Chinese Society of Agricultural Engineering, 2020, 36(23):124–130.
10. Xiaogang D, Lina M, Wenbo L, et al. Experimental study on the pore structure and soil-water characteristic curve of unsaturated remoulded weak expansive soil [J].Chinese Journal of Rock Mechanics and Engineering, 2022, 41(S1): 3081–3090. DOI: 10.13722/j.cnki.jrme.2021.0277.
11. Li X, Li L. Quantification of the pore structures of Malan loess and the effects on loess permeability and environmental significance, Shaanxi Province, China: an experimental study[J]. Environmental Earth Sciences, 2017, 76(15): 523.DOI: https://doi.org/10.1007/s12665-017-6855-7.
12. Raissi M, Perdikaris P, Karniadakis G E. Physics-informed neural networks: A deep learning framework for solving forward and inverse problems involving nonlinear partial differential equations[J]. Journal of Computational Physics, 2019, 378: 686–707.DOI:https://doi.org/10.1016/j.jcp.2018.10.045.
13. Karniadakis G E, Kevrekidis I G, Lu L, et al. Physics-informed machine learning[J].Nature Reviews Physics 2021.422-440.DOI:https://doi.org/10.1038/s42254-021-00314-5.
14. Raissi M, Perdikaris P, Karniadakis G E. Physics-informed neural networks: A deep learning framework for solving forward and inverse problems involving nonlinear partial differential equations[J]. Journal of Computational Physics, 2019, 378: 686–707.DOI:https://doi.org/10.1016/j.jcp.2018.10.045.
15. Wang S, Wang H, Perdikaris P. On the eigenvector bias of Fourier feature networks: From regression to solving multi-scale PDEs with physics-informed neural networks[J]. Computer Methods in Applied Mechanics and Engineering, 2021, 384: 113938.DOI:https://doi.org/10.1016/j.cma.2021.113938.
16. Lan P, Li H C, Ye X Y, et al. PINNs algorithm and its application in geotechnical engineering[J]. Yantu Gongcheng Xuebao, 2021.http://hdl.handle.net/10453/158294.
17. An R, Zhang X. Influence of dry and wet seasons on pore distributions of near-surface weathered granitic soil using mercury intrusion porosimetry and nuclear magnetic resonance imaging [J]. Authorea Preprints, 2023.DOI:https://doi.org/10.22541/essoar.168500312.22343407/v1.
18. L Wen-bo, N Gui-xia, M Li-na, et al. Microscopic Pore Structure Characteristics and Hydraulic Tortuosity of Unsaturated Remodeled Weakly Expansive Soil [J]. Journal of Changjiang River Scientific Research Institute, 2024, 41(04): 124–130+139.
19. Rigby S P, Edler K J. The influence of mercury contact angle, surface tension, and retraction mechanism on the interpretation of mercury porosimetry data [J]. Journal of Colloid and Interface Science, 2002, 250(1): 175–190.DOI:https://doi.org/10.1006/jcis.2002.8286.